Hierarchical porous N,O Co-doped carbon/Se composite derived from hydrothermal treated chitosan as Li–Se battery cathode

Chenhao Zhao[1,2] ✉, *Jiangshui Luo*[1,2], *Zhibiao Hu*[1,2]

[1]*Fujian Provincial Key Laboratory of Clean Energy Materials, Longyan University, Fujian Longyan 364012, People's Republic of China*
[2]*College of Chemistry and Materials, Longyan University, Fujian Longyan 364012, People's Republic of China*
✉ *E-mail: 3514983317@qq.com*

Published in Micro & Nano Letters; Received on 18th January 2018; Revised on 10th May 2018; Accepted on 8th June 2018

Seeking for the porous carbon with suitable structure and morphology has been a key to improve the lithium storage performance of carbon/selenium composite. In this work, the hierarchical porous N,O Co-doped carbon has been prepared by an initial hydrothermal carbonisation and subsequent activation route using the chitosan as raw material. The carbon obtained at 600°C possessing primary micropores and surface macropores presents high specific surface area (809. 3 $m^2 g^{-1}$) and low porous size, and the selenium with amorphous structure is uniformly encapsulated into the micropores of this carbon to form carbon/selenium composite. As the cathode materials of lithium ion battery, this composite delivers a discharge capacity of 446.9 mAh g^{-1} at rate of 0.24 C after 100 cycles. At a high rate of 4.8 C, this composite still shows a stable discharge capacity of 342.8 mAh g^{-1}. These results suggest that this composite may be promising for practical applications for lithium-selenium battery.

1. Introduction: In recent years, lithium-sulphur (Li–S) battery has become one of most promising candidates for next generation energy storage system due to its high discharge capacity (theoretical capacity: 1672 mAh g^{-1}) and low cost [1, 2]. However, the low electrochemical conductivity ($\sim 1 \times 10^{-28}$ S m^{-1}) of sulphur and serious 'shuttle effect' of soluble polysulphide compounds upon cycling result in low utilisation of active component, poor cycling stability and rate capability. As a congener of sulphur, the selenium (Se) also can be used as the cathode material of lithium ion battery based on similar lithium storage of sulphur ($2Li^+ + Se + 2e^- \leftrightarrow Li_2Se$). Importantly, the Se has an improved electron conductivity ($\sim 1 \times 10^{-3}$ S m^{-1}), much better than that of S [3–8]. Furthermore, the dissolution of polyselelide can be ignored in the carbonate base electrolyte [9], suggesting the Se will possess a better structural stability during cycling [3–9].

However, it has been proved that, the immediate use of pristine Se even nanosized Se, cannot have a good electrochemical performance as lithium ion battery cathode [10]. Referring to the design of Li–S battery cathode [2, 11], construction of Se/porous carbon composites has become a promising route to improve the electrochemical performance of Se [3–8, 12–16]. The carbon substrate can effectively elevate the electrochemical conductivity of Se, and buffer the volume change between the transformation of Se and Li_2Se. Also, the confined nanosized Se in the porous structure of carbon can increase its utilisation efficiency. For example, Zhang *et al.* have prepared porous carbon/Se composite form alkaline lignin, This composite electrode exhibits a reversible capacity of 596.4 mAh g^{-1} in the second cycle and a capacity retention of 453.1 mAh g^{-1} over 300 cycles with an average decay of 0.08% per cycle [17].

Therefore, it is essential to prepare the porous carbon substrate with high specific surface area and large porous volume. Chitosan $[C_6H_{11}NO_4)_n]$, a kind of bio-based polymers, made from shell of shrimps and other shell animals, has been widely used in the field of medicine, food and others. Also, it has been used as raw material to prepare porous carbon [18–20]. For example, a kind of hierarchical porous carbon has been prepared from chitosan/K_2CO_3 gel-like composite, and its specific surface can come to 2398.5 $m^2 g^{-1}$ [20]. However, some excessive organic solvent and equipment are necessary in the preparation process. In this Letter, an initial hydrothermal carbonisation and subsequent activation route has been developed to prepare chitosan derive porous carbon. The hydrothermal process help to destroy the polymer structure of chitosan and form any hydrophilic group on the surface of carbon, which is favourable for subsequent activation process [21, 22]. Then, carbon/selenium composite is made from above porous carbon. The structures and electrochemical performances of carbon and carbon/Se composite are clearly investigated in the text.

2. Materials and methods

2.1. Synthesis of hierarchical porous carbon: All reagents are A. R. grade and used without further purification. The hierarchical porous carbon is prepared by an initial hydrothermal carbonisation of chitosan and subsequent activation route described as follows: 2 g of chitosan is added into 75 mL distill water to form a suspension, and then is transformed into 100 mL polyphenylene linked autoclave. This system is kept at 210°C for 6 h. After cooling to room temperature, the obtained brown powder is collected by filtration, washed with deionised water and then ethanol for several times, and dried at 80°C in air. Two grams of brown powder are uniformly mixed with 4 g KOH, and the mixture is put into a corundum boat, and heat treated at 600°C for 2 h under nitrogen atmospheres with a heating rate of 5°C/min. The obtained black powder is ground in a mortar, washed with diluted hydrochloric acid until pH comes to 7, subsequent distill water and ethanol. Finally, the black carbon (denoted as 600-C) is dried at 80°C under air.

2.2. Synthesis of carbon/Se composite: 0.2 g of above carbon and 0.3 g of selenium powder (Aladdin China) is well mixed in an agate mortar using a small amount of ethanol as assistant. After the evaporation of ethanol, the Se/carbon composite is prepared using melting-diffusion route that heat treatment at 300°C for 6 h in a horizontal tube furnace under flowing Ar atmosphere.

2.3. Structure characterisation: XRD patterns are collected in a X-ray diffractometer (PANalytical X'Pert Powder XRD) at the scanning rate of 0.06°/s and 2θ degree of 10–80°. The morphologies, surface structure and element composition are observed by scanning electron microscope (SEM, Hitachi S3400, 5 kV). Specific surface area, pore size distribution and pore volume are

doi: 10.1049/mnl.2018.5154

derived from N_2 adsorption–desorption isotherms conducted in a as adsorption/desorption instrument (Micromeritics, USA). The Raman spectrum was obtained by Raman spectrometer (Renishaw, UK). Thermogravimetric analysis (TGA) measurements were carried out on a DSC200PC (Netzsch) at a heating rate of 10° C/min under N_2 atmosphere.

2.4. Electrochemical study: The electrochemical studies are performed by CR2016 coin cells. The working electrode is prepared by following procedure: carbon/Se composite, acetylene carbon and binder sodium alginate are uniformly mixed in a agate mortar at a weight ratio of 7:2:1. Then, the mixture is slurried by proper amount of water, and pasted onto the aluminium foils, dried at 80°C for about 5 h under air, and then cut into discs with a diameter of 14 mm. The lithium plate is used as counter and reference electrode. Polymer membrane (Celgarad 2400) and commercial $LiPF_6$ solution is used as separator and electrolyte, respectively. The average loading density of Se in the electrode can be calculated as ~1.20 mg cm^{-2}. The coin cells are assembled in an Ar-filled glove box, and three parallel cells are test for electrochemical performance. Galvanostatic cycling tests are carried out on a Neware CT-3008 battery test system within a voltage region of 1.0–3.0 V (vs. Li^+/Li) at different current densities.

3. Results and discussions

3.1. Structure and morphology: The chitosan-derived porous carbon is prepared by a hydrothermal carbonisation and subsequent activation route, and the carbon/Se composite is obtained by melting diffusion route at 300°C based on the melting point of selenium (221°C). The structures of 600-C, commercial Se and 600-C/Se composite are comparably studied by XRD and Raman spectrum (Fig. 1). Commercial Se shows a strong X-ray diffraction, and the diffraction peaks can be indexed to trigonal crystallinity Se. These diffraction peaks cannot be found in the 600-C/Se composite, suggesting the Se may experience a phase transformation from the crystallinity to amorphous upon the melting diffusion process. As for the Raman spectrum (Fig. 1*b*), 600-C or 600-C/Se has the Raman shifts called D (~1350 cm^{-1}, disordered carbon) and G band (~1580 cm^{-1}, graphitised carbon). The peak area ratio of D band to G band is 4.60 for 600-C, and this value can be kept stable (~4.51) for 600-C/Se composite. A Raman shift of 236.1 cm^{-1} is the characteristic of trigonal crystallinity Se, and this shift has disappeared in the 600-C/Se composite, which is the indicator of formed amorphous Se_8 ring [16, 17].

Fig. 2 reveals the N_2 adsorption–desorption isotherms and pores distribution curves of 600-C and 600-C/Se composite. The isotherm of 600-C can be indexed to type I isotherm according to IUPAC rule. The adsorption amount increases dramatically in a low pressure there, which can be attributed to the occupation of micropore and small mesopore. Then, the adsorption almost can be ignored until the coagulation of adsorption at a saturation pressure. The calculated BET-specific surface area of 600-C is 809.3 m^2 g^{-1},

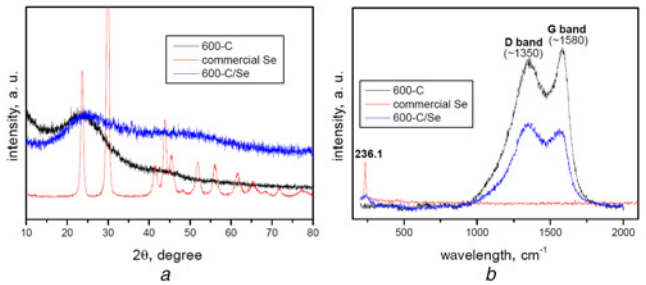

Fig. 1
a XRD patterns
b Raman spectrum of 600-C, commercial Se and 600-C/Se composite

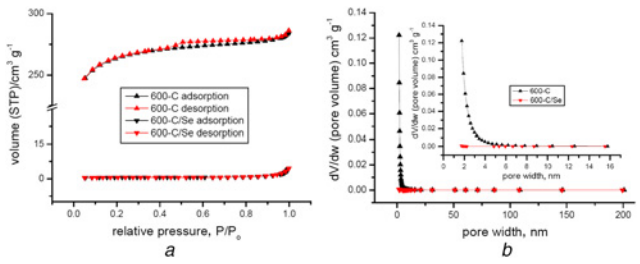

Fig. 2
a N_2 adsorption–desorption
b Pores distribution curves of 600-C and 600-C/Se composite, the inserted is pore distribution in the range of 0–10 nm

and the microporous volume also comes to 0.3340 cm^3 g^{-1}. The pore distribution of 600-C is in the range of 0–4 nm (Fig. 2*b*), indicating that these samples possess the micro- (<2 nm) and small meso-porous structure. According to previous literatures [5, 6], small porous structure is suitable for the encapsulation of selenium, and the confined selenium can present excellent electrochemical performance due to small size and effective buffer action during charge–discharge process.

The N_2 adsorption–desorption isotherm of 600-C/Se composite is presented in Fig. 2*a*. The composite presents a type II isotherm, and the adsorption of N_2 at low pressure almost can be ignored, indicating the composites does not have any microporous structure comparing with 600-C. In detail, the calculated BET-specific surface area of 600-C/Se composite is dramatically decreased to 1.77 m^2 g^{-1}, and the microporous volume is 5.0×10^{-4} cm^3 g^{-1}, resulting from effective occupation of confined amorphous Se in the microporous structure. As we know, the lower specific surface area of electrode materials can bring them fewer side reaction (a higher specific surface area means more reaction sites) and higher Coulombic efficiency upon cycling.

The SEM images of chitosan-derived porous carbon are revealed in Figs. 3*a* and *b*. The sample presents a 3D network structure with surface macropore in an overall view (Fig. 3*a*). Importantly, the formed macropore can provide pathway to diffusion of selenium in melting diffusion process [5]. In a close-up view (Fig. 3*b*), the surface of sample is smooth, and without any nanoparticle or defect can be observed.

In comparison with the carbon substrate, the morphology of 600-C/Se has any differences, especially, the structure turns to be

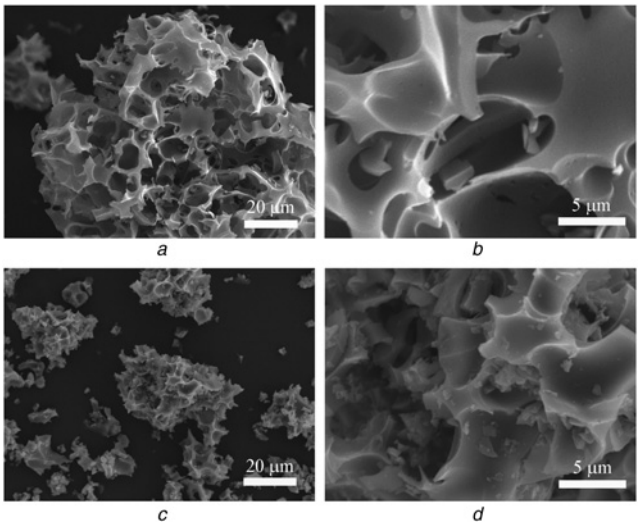

Fig. 3 *Overall and close-view SEM images*
a, *b* 600-C
c, *d* 600-C/Se composite

tighter (Fig. 3*c*). In a high magnification view, some broken segment can be found (Fig. 3*d*), which may be originated from long-time mixing process, observed in other literatures [16, 23].

In order to prove the occupation of confined amorphous Se in the microporous structure of carbon, the EDS mapping of 600-C/Se is shown in Fig. 4. It can be found that the Se or C element present a uniform distribution on the surface of carbon/Se composite, which is a great vindication that Se is confined in the pore of porous carbon, as discussed in Figs. 1 and 2. Furthermore, the overlap of O and N reflection also can be observed. The former one should be attributed to the incomplete carbonisation of O-contained chitosan, and the existence can help to combine with selenium based on same VI group elements by Van der Waals force [24]. Also, the N element originated from the branched chain of chitosan can increase the electrochemical conductivity and hydrophilic of carbon/Se composite [21, 22].

The chemical composition of 600-C is further studied by XPS, as shown in Fig. 5*a*. Three excitation peak can be indexed to the orbit of O1s, N1s and C1s, indicating the coexistence of C, N and O elements, originated from the backbone and side chain of chitosan. The surface atomic content of C, N and O element can be calculated as 87.8, 2.3 and 9.9%, respectively. Therefore, the as-prepared 600-C can be defined as porous N,O Co-doped carbon. TGA profile of 600-C/Se composite is revealed in Fig. 5*b*. A weight loss of ~16 wt% from 100 to 250°C can be found, which may be attributed to loss of partial adsorbed selenium. Then, a weight loss of ~34 wt% may be the loss of pore encapsulated selenium, and the actual selenium content of 600-C/Se should be ~50 wt%.

3.2. Electrochemical performance: As the cathode materials of lithium-selenium (Li-Se) battery, the electrochemical performances of 600-C/Se are clearly studied. Fig. 6 shows the typical discharge–charge curves and cycling stability of 600-C/Se composites at the rate of 0.24 C (based on the actual content of selenium, i.e. 50 wt%, 1 C = 675 mA g^{-1}). It delivers an initial discharge capacity of 987.7 mAh g^{-1}, and a reversible charge capacity of 579.8 mAh g^{-1} can be retained in subsequent charge (based on the actual selenium content, i.e. 50 wt%), correspondingly giving an initial Coulombic efficiency of 58.7%. In a typical discharge–charge curve (Fig. 6*a*), a discharge plateau of ~1.8 V corresponds the one-step reversible reaction of Se to Li_2Se. In the charge process, the platform is shifted to ~2.1 V, and the difference between charge and discharge process should be attributed the internal resistance of coin cell.

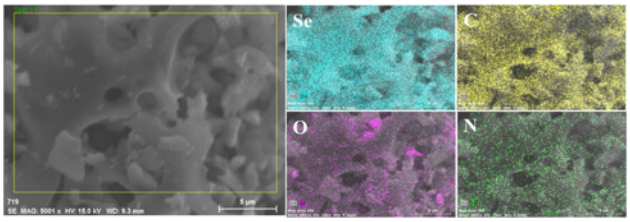

Fig. 4 *Selected area and Se, C, O and N mapping of 600-C/Se composite*

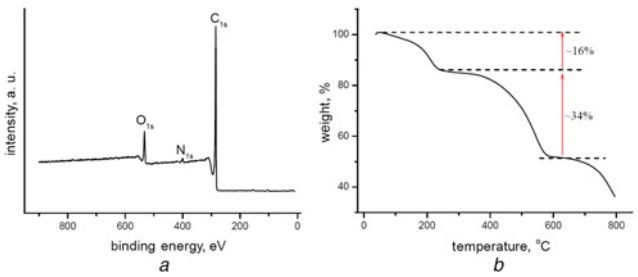

Fig. 5
a XPS spectrum of 600-C and
b TG analysis of 600-C/Se composite

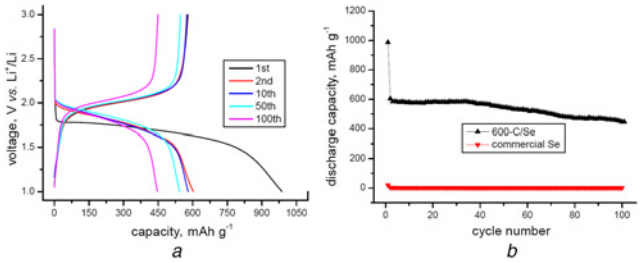

Fig. 6
a Typical charge discharge curves
b cycling stability of 600-C/Se composite at a current density of 0.24 C

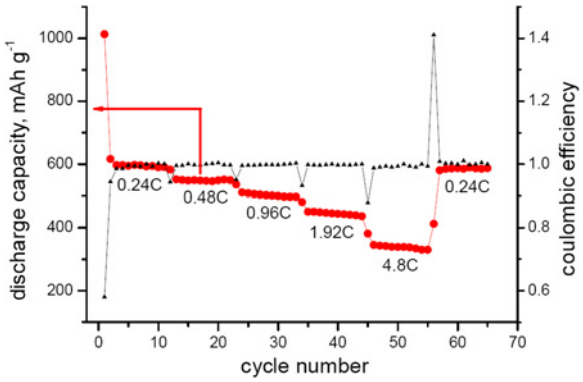

Fig. 7 *Rate capability and corresponding Coulombic efficiency of 600-C/Se at different current densities*

Cycling stability is shown in Fig. 6*b*, and the second reversible discharge capacity of 600-C/Se is 603.4 mAh g^{-1}, and a capacity value of 446.9 mAh g^{-1} can be retained after 100 continuous cycles. The capacity retention ratio comes to 74.1%. Importantly, the Coulombic efficiency of 100th cycle reaches 99.5%, indicating good electrochemical reversibility. By comparison, the commercial Se only delivers a discharge capacity of 1.1 mAh g^{-1} after 100 cycles due to large particle size of commercial Se (comes to ~75 µm).

Rate capability is another important parameter to weigh the electrode material. Fig. 7 shows the rate capability of 600-C/Se at different current densities. The discharge capacity decreases with increased current densities. The discharge capacity is 549.6, 506.0 or 450.4 mAh g^{-1} at the rate of 0.48, 0.96 or 1.92 C, respectively. Even at a high rate of 4.8 C, the composite electrode still delivers a stable discharge capacity of 342.8 mAh g^{-1}. Interestingly, when the rate comes back to 0.2 C, the discharge capacity also goes back to 487.3 mAh g^{-1}. Also, the Coulombic efficiency (the ratio of charge capacity to discharge) of 600-C/Se slightly increases upon cycle. After 60 cycles, the efficiency value can exceed 99% for each cycle. These results prove that the 600-C/Se composite has good rate capability, and can be used at high current density.

4. Conclusions: A hydrothermal-assisted carbonisation and subsequent activation route has been developed for preparation of chitosan-derived hierarchical porous carbon, which is used as substrate for carbon/Se composite. As cathode of Li-Se battery, the 600-C/Se composite can deliver a discharge capacity of 603.4 mAh g^{-1} at 0.24 C, and possesses good cycling stability and rate capability. The improved electrochemical performances should benefit to high specific surface area, low porous size and

doi: 10.1049/mnl.2018.5154

3D structure of 600-C. Maybe, this hierarchical porous carbon can be used in the fields such as catalysis and adsorption.

5. Acknowledgments: The authors thank the financial supports from the Scientific Start Foundation of LongYan University (grant no. LB2014001), from Provincial Science and Technology Department for Provincial Colleges and Universities Program (grant no. JK2015047).

6 References

[1] Evers S., Nazar L.F.: 'New approaches for high energy density lithium-sulfur battery cathodes', *Acc. Chem. Res.*, 2013, **46**, pp. 1135–1143

[2] Manthiram A., Yu F., Su Y. F.: 'Challenges and prospects of lithium-sulfur batteries', *Acc. Chem. Res.*, 2013, **46**, pp. 1125–1134

[3] Abouimrane A., Dambournet D., Chapman K.W., *ET AL.*: 'A new class of lithium and sodium rechargeable batteries based on selenium and selenium–sulfur as a positive electrode', *J. Am. Chem. Soc.*, 2012, **134**, pp. 4505–4508

[4] Yang C.P., Yin Y.X., Guo Y.G.: 'Elemental selenium for electrochemical energy storage', *J. Phys. Chem. Lett.*, 2015, **6**, pp. 256–266

[5] Jin J., Tian X.C., Srikanth N., *ET AL.*: 'Advances and challenges of nanostructured electrodes for Li–Se batteries', *J. Mater. Chem. A*, 2017, **5**, pp. 10110–10126

[6] Eftekhari A.: 'The rise of lithium–selenium batteries', *Sust. Energy Fuels*, 2017, **1**, pp. 14–19

[7] Xu J.T., Ma J.M., Fan Q.H., *ET AL.*: 'Recent progress in the design of advanced cathode materials and battery models for high-performance Lithium-X (X=O_2, S, Se, Te, I_2, Br_2) batteries', *Adv. Mater.*, 2017, **29**, p. 1606454

[8] Zeng L.X., Chen X., Wei M.D.: 'Green synthesis of a Se/HPCF–rGO composite for Li–Se batteries with excellent long-term cycling performance', *J. Mater. Chem. A*, 2017, **5**, pp. 22997–23005

[9] Cui Y.J., Abouimrane A., Sun C.J., *ET AL.*: 'Li-Se battery: absence of lithium polyselenides in carbonate based electrolyte', *Chem. Commun.*, 2014, **50**, pp. 5576–5579

[10] Liu L.L., Hou Y.Y., Wu X.W., *ET AL.*: 'Nanoporous selenium as a cathode material for rechargeable lithium–selenium batteries', *Chem. Commun.*, 2013, **49**, pp. 11515–11517

[11] Li W.F., Liu M.N., Wang J., *ET AL.*: 'Progress of lithium/sulfur batteries based on chemically modified carbon', *Acta Phys. Chim. Sin.*, 2017, **33**, pp. 165–182

[12] Liu T., Zhang Y., Hou J.K., *ET AL.*: 'High performance mesoporous C@Se composite cathodes derived from Ni-based MOFs for Li–Se batteries', *RSC Adv.*, 2014, **5**, pp. 84038–84043

[13] Wang X.W., Zhang Z.A., Qu Y.H., *ET AL.*: 'Solution-based synthesis of multi-walled carbon nanotube/selenium composites for high performance lithium–selenium battery', *J. Power Sources*, 2015, **287**, pp. 247–252

[14] Hong Y.J., Kang Y.C.: 'Selenium-impregnated hollow carbon microspheres as efficient cathode materials for lithium-selenium batteries', *Carbon*, 2017, **111**, pp. 198–206

[15] Liu T., Jia M., Zhang Y., *ET AL.*: 'Confined selenium within metal-organic frameworks derived porous carbon microcubes as cathode for rechargeable lithium–selenium batteries', *J. Power Source*, 2017, **341**, pp. 53–59

[16] Zhang H., Yu F. Q., Kang W. P., *ET AL.*: 'Encapsulating selenium into macro-/micro-porous biochar-based framework for high-performance lithium-selenium batteries', *Carbon*, 2015, **95**, pp. 354–363

[17] Zhang H., Jia D.D., Yang Z.W., *ET AL.*: 'Alkaline lignin derived porous carbon as an efficient scaffold for lithium-selenium battery cathode', *Carbon*, 2017, **122**, pp. 547–555

[18] Fujiki J., Yogo K.: 'The increased CO_2 adsorption performance of chitosan-derived activated carbons with nitrogen-doping', *Chem. Commun.*, 2016, **52**, pp. 186–189

[19] Olejniczak A., Lezanska M., Lukaszewicz J. P.: 'Novel nitrogen-containing mesoporous carbons prepared from chitosan', *J. Mater. Chem. A*, 2013, **1**, pp. 8961–8967

[20] Chen C., Liu K.Y., Zhao C.H.: 'Synthesis of Se/chitosan derived hierarchical porous carbon composite as Li-Se battery cathode', *Funct. Mater. Lett.*, 2017, **10**, p. 1650074

[21] Deng J., Li M.M., Wang Y.: 'Biomass-derived carbon: synthesis and applications in energy storage and conversion', *Green Chem.*, 2016, **18**, pp. 4824–4854

[22] Wang J., Nie P., Deng B., *ET AL.*: 'Biomass derived carbon for energy storage device', *J. Mater. Chem. A*, 2017, **5**, pp. 2411–2428

[23] Zhao C.H., Xu L.B., Hu Z.B., *ET AL.*: 'Facile synthesis of selenium/potassium tartrate derived porous carbon composite as an advanced Li–Se battery cathode', *RSC Adv.*, 2016, **6**, pp. 47486–47490

[24] Ye H., Ye Y.X., Guo Y.G.: 'Advanced Se–C nanocomposites: a bifunctional electrode material for both Li–Se and Li-ion batteries', *J. Mater. Chem. A*, 2014, **2**, pp. 13293–13298